A porous geopolymer based on aluminum-waste with acoustic properties

C. Leiva, *Y. Luna-Galiano, C. Arenas, B. Alonso-Fariñas, C. Fernández Pereira

University of Seville, School of Engineering, Chemical and Environmental Engineering Department, Camino de los Descubrimientos s/n 41092, Seville (Spain), (0034-954481180, Fax: 0034-954486082, yluna@us.es)

Abstract

Paval, a solid waste stream from the aluminum industry, is used as a pore generation agent in geopolymers. Paval was mixed with coal combustion fly ash, as a geopolymeric precursor, and activated with alkaline solution with the aim of obtaining porous geopolymers to be used as noise barriers. Both geopolymeric and pore generation reactions happen simultaneously. Aluminum from Paval can react with water and OH^- from the geopolymerization activating solution, producing hydrogen. The hydrogen gas released generates a highly porous material. The influence of the fly ash-paval proportion and the setting temperature on open porosity, compressive strength and noise-absorbing properties were evaluated. To better understand these influences, the setting time, volume expansion and mineral composition were also studied. The obtained results showed that a higher Paval content (fly ash-Paval ratio 50:50) and setting temperature (70 ºC) produced a lower setting time and higher volume expansion, increasing the open porosity and improving acoustic properties, but reducing the compressive strength. The material manufactured under these conditions showed similar amorphous phase content to the non-porous geopolymers made

without Paval. On the other hand, the obtained materials did not raise environmental concerns in a normalised leaching test.

Keywords: fly ash, geopolymer, aluminum wastes, pore generation, sound absorption

1. Introduction

Foam concrete is considered a lightweight material with a high degree of void space (high porosity) in its matrix (Zhang et al., 2014) which may find applications in some areas of the construction field where thermal and acoustic insulation properties are required (Hajimoohammadi et al 2017). Accordingly, porous geopolymers appear a more eco-friendly alternative than conventional porous concretes made from cement. Geopolymers are the hardened products after the activation of solid aluminosilicates with an alkaline solution at room (or slightly higher) temperature (Davidovits, 1991). There are two general methods to generate pores in geopolymers (or in any cementitious material) (Bai and Colombo, 2018). On the one hand, using chemical agents (Arellano Aguilar et al., 2010, Hlaváček et al., 2015, Prud'homme et al., 2010, Prud'homme et al., 2011, Kränzlein et al., 2018, Papa et al., 2016, Bai et al., 2019), which reacts generally in an alkaline medium producing gas bubbles that get trapped during the hardening of the geopolymer (Luna-Galiano et al., 2018). On the other one, using mechanical agents such as surfactants, which release air bubbles during mixing (Cilla et al., 2014-1, Masia et al., 2014, Xu et al., 2018, Hassan et al., 2018). In general, a reactive metal powder (Al) reacts with water and hydroxide in an alkaline environment producing bubbles of hydrogen gas and hydrolysed metal complexes (Zhang et al., 2014, Mohammadian and Haghi, 2013, Mufasa Al Bakri et

al., 2011, Kränzlein et al., 2018). These bubbles attempt to escape into the air from the geopolymer paste causing the expansion of the geopolymer mortar (Neville, 2011) and generating the porous structure. There are several studies about the generation of pores in geopolymers using Al powder as pore generation agent (Arellano Aguilar et al., 2010, Hlaváček et al., 2015, Hajimoohammadi et al., 2017, Kamseu et al., 2012, Kränzlein et al., 2018) or using recycled aluminum powder (Font et al., 2017, Dembovska et al., 2017). These works have studied the geopolymerization and chemical pore generation reaction, kinetics and physical (porosity), mechanical (compressive strength) and thermal (conductivity) properties. However, the use of aluminum powder involves an increase in the cost of the material manufacture. For this reason, in this research a high- aluminum-content waste stream generated in the recycling process of salt slag from the aluminum industry (secondary aluminum), called Paval (García Serrada, 2002), is used as aluminum source for pore generation. This material is composed of a mixture of different aluminum compounds (Al^0, Al_2O_3), silicon (SiO_2) and Fe, Mg, Ca and Na compounds. Its chemical composition is variable, depending on the composition and quality of the raw materials, the collection system and the classification procedure (López Gómez, 2005). It shows potential applications in several fields (cement, concrete, refractory, ceramics, and steel industry). Some authors (García Serrada, 2002) have studied the use of Paval as a filler in the manufacture of hot bituminous mixtures. Tayibi et al. studied (Tayibi et al., 2016) the production of low reactive aggregates by means of setting Paval with gypsum in order to simplify the handling and the transport of aggregates. López-Delgado et al. (López-Delgado et al., 2009) specified the production of calcium aluminosilicate inert glass from the fusion at 1500ºC of mixtures of sand, calcium carbonate and Paval. Other works

(Gonzalo Delgado, 2008, Gonzalo Delgado et al., 2011) have studied the recovery of the aluminum from the waste using a hydrothermal method at a low temperature in order to revalue it.

One of the main applications of porous materials is as an acoustic absorbent since they are able to attenuate the sound waves, increasing air resistance by means of the impact of sound in the porous structure (Han et al., 2003). These materials can be used to reduce the noise pollution, an environmental problem that is becoming an increasingly significant concern due to its negative impact on human health.

The current work has a dual environmental design. 1) to recycle industrial wastes generated in high amounts: Fly ashes from coal combustion, whose European production was higher than 145 million of tonnes in 2014 (Ahmed et al., 2016), were used as geopolymerization raw material; Paval was used as a pore generation agent and his European production was 360000 tonnes per year after recycling 1 million of tonnes of salt slags (Basque Eco design Meeting, 2017). 2) to develop an acoustic absorbing material in order to reduce traffic noise pollution levels. With the aim of achieving the greatest acoustic absorbing behaviour of the product, two parameters have been studied: the fly ash-Paval proportion and the setting temperature.

2. Materials and methods

2.1 Materials

The solid geopolymeric precursor was a low calcium fly ash (FA) (ASTM class F (ASTM C618-05, 2005)) from a coal combustion power plant. Paval (PV) was used as an aluminum

source. The chemical composition of both materials (Table 1) was determined after chemical attack and dissolution at 750 ºC (ASTM D-3682-78) (ASTM D3682-78, 1983) using atomic absorption spectroscopy. Minor elements (Table 2) were determined by means of inductively coupled plasma-atomic emission spectrometry. The specific gravity, in accordance with EN 1097-7 (EN 1097-7, 2009), was also determined. PV and FA showed values of 2.51 g/cm^3 and 1.93 g/cm^3, respectively, for specific gravity.

Table 1. Chemical composition of FA and PV

High content of both SiO_2 and Al_2O_3 was observed in FA. Since PV is an aluminum industry waste, it exhibited a high Al content.

The high Ba content and the medium values of Zn, Cr, Ni and V in the FA were noteworthy. PV is a by-product with a higher metal content than the FA in this study. Mo, Zn, Pb, Cr, Ni, Cu, Ba, Sn and Se contents were also evident in PV. Both materials were subjected to the UNE-EN 12457-4 leaching test (Table 2). Leachate pH values were 11.5 and 9.3 for FA and PV respectively. Metal concentrations and European Landfill Directive (EULFD) limits of Inert Waste (IW), Non-hazardous Waste (NHW) and Hazardous Waste (HW) were detailed too. Most of the metals were under the IW limits, except Cr and Se in FA and Mo in FA and PV. It is necessary to carry out a leaching test on the geopolymers to evaluate the environmental impact of the final product due to these high metal concentrations.

110 Table 2. Minor elements and metal concentrations obtained after UNE EN 12457-4
111 leaching test of FA and PV.

112

113 Raw materials (FA and PV) were also evaluated by means of X-ray powder diffraction
114 (XRD) in order to study their mineral composition. AD8 Advance A25 (BRUKER) (40 kV
115 and 30 mA) equipment was used. Phase identification and amorphous content were
116 performed using the DIFFRAC.EVA software (BRUKER). XRD patterns are shown in
117 Figure 1. FA showed certain amorphous grade, demonstrating a slight broad peak between
118 15-38 values of 2θ. Estimated amorphous content was 44.1 %. Quartz and mullite were the
119 main crystalline peaks detected in FA. In contrast, PV showed a lower amorphous content
120 (26.3 %) than FA (44.7%). Corundum, bayerite, ringwoodite, norstrandite and kogarkoite
121 were the main crystalline phases detected in PV.
122 Figure 1. XRD patterns of FA, PV and geopolymers FA100-PV0 and FA50-PV50

123

124 The particle size distribution of raw materials was determined using a laser diffraction
125 granulometer provided by Micromeritics. FA presented the finest particle size distribution
126 with D10, D50 and D90 of 1.49, 12.57 and 42.27 μm respectively. PV was the coarsest
127 material of both with D10, D50 and D90 of 2.51, 50.07 and 334.7 μm respectively. A wide
128 particle size distribution, with compensation between fractions, and percentages of 80-90 %
129 for particle sizes less than 45 μm are considered the suitable particle size distribution in raw
130 materials for geopolymerization (Geoash Project, 2004-2007).

131 The activating solution used in the geopolymer manufacture was prepared with potassium
132 silicate (SiO_2 23 wt % and K_2O 14.9 wt %) (supplied by Industrias Químicas del Ebro) and
133 enough potassium hydroxide to increase the K_2O/SiO_2 molar ratio up to 1.1 (pH of solution
134 is 13.3).

135 **2.2 Geopolymer preparation**

136 Geopolymers were prepared in a laboratory mixer (5 kg capacity) working at 500 rpm. First
137 of all, FA and PV were mixed for 2 minutes. Secondly, activating solution was added to the
138 solid until a workable paste with thixotropic behaviour was obtained (mixing time around 4
139 minutes). Geopolymer samples were moulded in 35 mm-diameter and 80 mm-high
140 cylinders plastic moulds and filled to 40 mm-high in order to allow for the expansion of the
141 material.

142 Three geopolymers samples were manufactured. Geopolymer sample FA100-PV0 was
143 prepared without paval. The final product was a non-porous geopolymeric paste.
144 Geopolymers FA75-PV25 and FA50-PV50 were prepared with the proportion FA:PV
145 specified in their name and the final product after geopolymerization was a porous material.
146 These three geopolymer materials were set at 40 ºC for 24 hours. After setting, they were
147 demoulded and cured at room temperature (average temperature: 20 ºC; average relative
148 humidity: 45 %) for 28 days. One more geopolymer (FA50-PV50) were prepared and set at
149 70 ºC for 24 hours, in order to study the influence of setting temperature. As FA was
150 replaced by PV, the amount of activating solution needed to obtain a thixotropic and
151 workable paste was slightly reduced. Geopolymer sample FA100-PV0 needed 0.52 g

activating solution per gram of solid phase and geopolymers FA75-PV25 and FA50-PV50 needed 0.51 and 0.49 g activating solution per gram of solid phase respectively. In order to maintain the same water proportion, water additions were carried out during the preparation of geopolymers with Paval. FA75-PV25 and FA50-PV50 needed 0.006 and 0.016 g of water per gram of solid phase respectively. The authors tried to prepare one sample mixing paval (without fly ash) with the activating solution but the paste was neither workable nor thixotropic enough.

When porous geopolymers had expanded along the mold of 80 mm in height during setting, samples were cured for 28 days, and were then cut with a saw at 40 mm in height in order to have the same length for the measurement of open porosity, compressive strength, acoustic properties and leaching behavior.

2.3. Methods

Geopolymerization reaction and pore generation reactions must be evaluated in order to study how both reactions could affect the properties of the final products. As FA and PV are mixed with the activating solution, two reactions take place: the geopolymerization reaction and the pore generation reaction. The geopolymerization reaction happens when FA reacts with the activating solution generating different coexistent geopolymeric gels (N-A-S-H, K-A-S-H) which harden and produce the geopolymer structure. The type of gel depends on the activating solution and the chemical composition of the raw material (Fernández-Jiménez et al., 2006). As fly ash is activated with potassium silicate, the main gel obtained is K-A-S-H (potassium aluminate silicate hydrate) gel (Fernández-Jiménez et

al., 2006, Luna-Galiano et al., 2016). The pore generation reaction occurs as metallic aluminum reacts with water (Mohammadian and Haghi, 2013) or alkali (Al Bakri et al., 2011), according to the following reactions:

-Aluminum with water (Mohammadian and Haghi, 2013),

$2Al + 6H_2O \rightarrow 2Al(OH)_3 + 3H_2$ (reaction 1)

$2Al + 3H_2O \rightarrow Al_2O_3 + 3H_2$ (reaction 2)

-Aluminum with alkali (Na or K) hydroxides (Al Bakri et al., 2011),

$2Al\ (s) + 2OH^-\ (aq) + 6H_2O\ (l) \rightarrow 2Al(OH)_4^-\ (aq) + 3H_2\ (g)$ (reaction 3)

The first and second reactions lead hydrogen and aluminum hydroxide and aluminum oxide respectively. Both reactions are highly exothermic and thermodynamically favorable from room temperature to 660 ºC (Digne et al., 2002).

The third reaction produces $Al(OH)_4^-$ from Paval, so more $Al(OH)_4^-$ appears in the medium available to condensate, and therefore the interaction silicate-aluminate species could predominate instead interaction silicate-silicate (De Silva et al., 2007).

2.3.1. Volume expansion and setting time

Setting time was determined in order to evaluate the kinetics of the geopolymerization reaction. This parameter was measured in accordance with the EN 196-3 (EN 196-3, 2005) using a Vicat needle. The expansion volume (mm) of the geopolymer during the setting was also measured in order to assess the kinetic of the pore generation reaction. The ratio between the volume of the material at instant t, V(t), and the initial volume of introduced paste, V(0), were the parameters used to identify the expansion volume.

2.3.2. XRD analysis

195 Geopolymer samples were also evaluated by means of X-ray powder diffraction (XRD) in
196 order to study their mineral composition and to evaluate the crystalline and amorphous
197 contents. The amorphous content is one of the key factors to consider because it gives an
198 idea of the extent of the geopolymerization reaction (Fernández-Jiménez and Palomo,
199 2003).

200 **2.3.3. Physical and mechanical properties**

201 Open porosity is deeply linked with the acoustic properties of a material. Open porosity
202 was determined using the vacuum water saturation method (EN 1936, 2006). Compressive
203 strength of geopolymer was measured using a compressing test machine (Tinius Olsen-
204 TO317EDG). The compressive strength tests were performed in accordance with EN 196-1
205 (EN 196-1, 2006). Four specimens of each type of geopolymers were used to determine
206 these properties.

207 **2.3.4. Acoustic properties**

208 The acoustic properties of the geopolymeric materials were evaluated measuring the sound
209 absorption by the transfer-function method described in EN ISO 10534-2 (EN ISO 10534-
210 2, 1998). An impedance tube (Kundt tube) was used. The arithmetic mean of the absorption
211 coefficients (α) at 250 Hz, 500 Hz, 1000 Hz and 2000 Hz, and the Noise Reduction
212 Coefficient (NRC) were determined. Three specimens of each geopolymer have been
213 evaluated. The specimens are placed in the Kundt tube in such a way that the incident
214 sound wave penetrates the material from the more porous zone (upper zone in Figure 3e) to
215 the less porous zone (bottom zone in Figure 3e).

216 **2.3.5. Leaching test**

Given that the fly ash and the aluminum by-product (Paval) are residual materials with a high hazardous metal content, a leaching test study has been carried out in order to complete the characterization of the final product. A metal stabilization process may happen during the geopolymerization reaction, so it is necessary apply a leaching test resembling reality, e.g. waste in a landfill with rainwater acting on the surface of a monolith. For this reason, geopolymers were subjected to one of the most commonly tests for monolith samples in the waste management field in Europe, the NEN 7345 tank leaching test (NEN 7375, 2005) which uses water as a leach fluid. The leachates were also measured in the General Research Services of the University of Seville (CITIUS) using ICP-OES equipment. Cumulative metal concentrations (mg/m^2) in the leachates were compared with the Dutch Decree on Soils Quality (DSQ) limits (DSQ, 2007).

3. RESULTS AND DISCUSSION

The obtained results are presented and discussed in this section in order to analyse the influence of both the FA:PV ratio and setting temperature on the properties of the geopolymeric foam.

3.1. Setting time and expansion volume results

Figure 2 represents the setting curves (as Vicat needle penetration percentages) over time of the geopolymers (Set curves). Curves show three stages. The first stage represents the plastic period of the setting in which the material has not started to set. The second stage is the setting period of the material (material shows needle penetration resistance over time).

238 The final step corresponds to the hardening period. The geopolymer (FA100-PV0)
239 (prepared without Paval) showed an initial and final setting time of around 15 and 20 h,
240 respectively.
241 Figure 2. Expansion volume and setting curves
242
243 As fly ash was replaced by Paval, a reduction of setting time was observed. Geopolymer
244 FA50-PV50 exhibited an initial and final setting time of around 4 and 7 hours, respectively.
245 In order to explain this fact, the Si/Al ratio in the raw material should be taken into account
246 since it is a parameter which plays an important role in the setting and final stages strength
247 (De Silva et al., 2007). Al appears to control the setting of geopolymers. When the Si/Al
248 ratio is around 1, a quick set is observed. However, when the Si/Al ratio is higher than 1,
249 the development of reactions is slow. Systems with high Si/Al ratios could produce more
250 $Al(OH)_4^-$ in the medium available to condensate. The condensation rate between
251 aluminate-silicate species is higher than silicate-silicate species (De Silva et al., 2007), with
252 the consequence of an increase in setting time. In this work, samples FA100-PV0, FA75-
253 PV25 and FA50-PV50 have an initial Si/Al molar ratio of 2.53, 1.92 and 1.33, respectively.
254 As can be seen, the substitution of FA with PV produced a decrease in Si/Al in the system
255 which explained the reduction in the setting time. Setting temperature also affected to the
256 setting rate. Setting time was reduced when working at 70 ºC rather than 40 ºC because the
257 higher temperatures (60-80 ºC) increase the dissolution of silica and alumina that
258 participate in the geopolymerization reaction (Ahmer et al., 2016).
259 Figure 2 also shows the expansion volume natural logarithm of geopolymers (EV curves).
260 The geopolymer FA100-PV0 did not show expansion volume. However, as Paval was

added to the mixture, an increase in the geopolymer volume was evident. This increase in volume was due to the H_2 gas released during reactions 1-3. As can be seen, as Paval content was increased, the expansion volume increased since there was more Al in the mixture to produce reactions 1-3. In addition, setting at 70 ºC instead of 40 ºC also produced a rise in expansion volume due to the positive effect of the temperature in the kinetics of pore generation reaction (H_2 generation) (Henon et al., 2013).

All expansion volume curves have the same shape (tilted s-shape). There was a period of time in which expansion volume was null. This period is known as the latency period (Luna-Galiano et al., 2018, Henon et al., 2013). After that, the expansion volume started to grow (mainly linearly) due to the release of gas. Finally, expansion volume remained steady over time. As can be seen, the use of Paval in a proportion of 25 wt% produced an expansion of volume in the material, which begun at 8 hours. The expansion of volume started at 4 hours when the proportion of Paval was 50 wt%. In this case, the expansion was greater. In addition, when th setting temperature was 70 ºC the expansion of volume started at 1 hour and the expansion volume continued growing. These expansion volume results are related to the production of gas (H_2(g)) from reactions 1-3.

Analyzing the "Set" and "EV" curves in Figure 2, it can be seen that PV content and setting temperature affected the latency period (EV curves) as well as the plastic period (Set curves), reducing both times in such a way that both practically matched. In addition, the linear period of expansion volume (EV curves) and the setting period (Set curves) also matched, which is related to the behavior of a bubble in a fluid-plastic medium. When a gas bubble is generated within the geopolymer it tries to escape from the material to the air. If the geopolymer has high fluidity (plastic period of setting), gas bubbles can escape easily.

During the setting period, paste loses fluidity and the gas produced cannot escape from the material because it is trapped in the hardening matrix, producing an expansion of the geopolymer. So, although H_2 gas is produced from the initial time, it does not produce expansion of the material until the material starts to set. If the reaction of geopolymerization is quick, it is possible to match up the geopolymerization reaction and gas generation reaction. However, if geopolymerization reaction is slow, gas generated during the reaction is practically released. Therefore, controlling the geopolymerization and pore generation reaction rate, it is possible to develop geopolymers with a certain degree of porosity.

3.2. XRD

Figure 1 also shows the XRD patterns of the geopolymers FA100-PV0 and FA50-PV50. These patterns have been compared with the raw material patterns (Figure 1) in order to understand the changes that happened in the raw materials during geopolymerization.
As can be seen, there are few differences between FA and geopolymer FA100-PV0. FA showed a slight broad reflection in the 2θ range 15-38 with crystalline peaks of quartz and mullite. Geopolymer FA100-PV0 showed a slight shift of the broad peak in the 2θ range (22-38) with respect to FA pattern, which proves the dissolution of SiO_4 and AlO_4 species during the geopolymerization reaction (Prud`homme et al., 2010). Quartz and mullite peaks in the geopolymer FA100-PV0 were in the same 2θ position as the FA pattern but their intensities were lower, which indicates a lower degree of crystallinity in the geopolymer than in the fly ash, so some alteration of crystal structure may have taken place (Prud`homme et al., 2011).

When FA was replaced by PV, certain changes were observed in the geopolymer FA50-PV50 pattern with respect to the geopolymer FA100-PV0 pattern. Quartz and mullite were observed in the FA50-PV50 pattern, which come from the fly ash. Their intensities in FA50-PV50 were slightly lower than in FA100-PV0 due to the smaller proportion of FA in the mixture. In addition, other crystalline phase peaks appeared in the geopolymer FA50-PV50 (corundum, bayerite, norstrandite), corresponding to the PV crystalline phases, but with much lower intensities than PV. Despite these other crystalline phases, FA100-PV0 and FA50-PV50 showed similar amorphous phase contents (53.6 and 52.1 % respectively (calculated using the DIFFRAC.EVA software)), with the same broad peak position. FA100-PV0 only undergoes the geopolymerization reaction, so the amorphous content of the initial formulation was the amorphous content of FA, i.e. 44.7 %. After geopolymerization, the amorphous content was 53.6 %, i.e. 8.9 point increase. The FA50-PV50 sample started with an amorphous content of 35.5 % (average between 44.7 and 26.3 % amorphous content of FA and PV, respectively) and after geopolymerization+pore generation reactions reached an amorphous content of 52.1 % (16.6 point increase). This involves two things: firstly, the geopolymerization reaction extension in sample FA100-PV0 and geopolymerization+pore generation reaction extensions in sample FA50-PV50 are quite similar, slightly higher in the formulation of FA100-PV0. Secondly, the extent of the reaction of geopolymerization+pore generation is not as low as expected. Taking into account that FA is the main reactive agent in the geopolymerization (PV did not geopolymerize) and the amount of FA is less in FA50-PV50, it seems that the increase in amorphous content in this sample is also due to the pore generation reaction. In order to explain this fact, it is necessary to analyze the reactions of pores generation (reaction 1-3).

329 Reaction 1 forms $Al(OH)_3$. This reaction is based on the reaction of amalgamated
330 aluminum with water at room temperature (Pereira Antunes et al., 2002), which uses the
331 method of Schmäh (Schmäh, 1946) for bayerite preparation. A precipitate of non-
332 crystalline aluminum hydroxide is formed in first place, which crystalize to form bayerite.
333 This crystallization takes place after 20-30 h at room temperature (Pereira Antunes et al.,
334 2002). In the current work, geopolymer FA50-PV50 set at 5 hours, so there was no time to
335 form bayerite by means of the Schmäh method. The slight presence of bayerite in theFA50-
336 PV50 pattern supports this behavior and therefore could explain the amorphous content of
337 the geopolymer prepared with PV.

338 **3.3. Open porosity**

339 Effects of PV content and setting temperature on open porosity are shown in Table 3. As
340 can be seen, open porosity increased as PV content and setting temperature were increased.
341 These results are closely connected to the volume expansion values (Figure 2) since the
342 higher the volume expansion, the higher the open porosity, that is, a more developed porous
343 geopolymer was obtained. The evolution of bulk density was opposite to open porosity, i.e.
344 it decreased as FA was replaced by PV, with PV content and setting temperature.
345 Table 3. Open porosity and compressive strength
346
347
348 Figure 3 shows photographs visualizing the pore size generated after the
349 geopolymerization-pore generation reaction. Geopolymer FA100-PV0 (Figure 3a) did not
350 show visible porosity. Geopolymer FA75-PV25 (Figure 3b) showed visually appreciable

pores, with sizes less than 3 mm. Geopolymer FA50-PV50 (Figure 3c) exhibited higher pore proportion than FA75-PV25, with sizes less than 5 mm and certain connectivity between pores. Geopolymer FA50-PV50 set at 70 ºC (Figure 3d), revealed the greatest open porosity and pore sizes, some of these higher than 5 mm.

These high pores appear when small bubbles ascend and begin to coalesce during the setting time, which produced an improvement in the connectivity between pores. In general, pore sizes obtained with the introduction of Paval were in the range 1-7 mm. The range 1-5 mm is considered the most suitable for acoustic absorbing materials (Flores, 1990). Figure 3e) shows the cross section of geopolymer FA50-PV50 cured at 70 ºC. As can be seen, the generation of bubbles produced a highly tortuous macro-porous network. This network is formed by large and irregular pores connected by small pores located in the pore walls (Papa et al., 2016), which form a complex channel structure acting as a Helmholtz´s resonator. As can be observed, this structure was more macro-porous in the upper zone than in the bottom zone (due to the coalescence commented upon before). This change in the overall porous structure (low-porous-bottom zone vs high-porous-upper zone) causes the global channels network to appear as a system where the sound wave may enter but not leave.

Figure 3. Geopolymer images and cross section of FA50-PV50 70ºC

3.4. Compressive strength

372 Values of compressive strength at 28 days of curing are detailed in Table 3. Compressive
373 strength of the geopolymer without Paval (FA100-PV0) was 14.8 MPa. When paval was
374 introduced into the formulation the compressive strength reduced significantly (to 5.32
375 MPa with 25 % Paval and 4.23 MPa with 50 % Paval). The setting temperature also
376 affected the compressive strength: FA50-PV50, set at 70 ºC, showed a compressive
377 strength value of 3.07 MPa. These results are consistent with the open porosity values. In
378 general, a highly porous material (high porosities with the rest of parameters constant)
379 displais reduced mechanical properties due to the lower volume/mass ratio (Luna-Galiano
380 et al., 2018). Font et al., (Font et al., 2017) prepared geopolymer eco-cellular concretes
381 (GECC) with fluid catalytic cracking catalyst residue (FCC) as a raw material and additions
382 of recycled aluminum foil powder as pore generating agent and compared with the use of
383 Al powder. GECC with recycled aluminum and Al powder showed a compressive strength
384 of 3.5 MPa (density of 690 kg/m^3) and 1.87 MPa (density of 590 kg/m^3), respectively, at 7
385 days of curing. Work carried out by Dembovska (Dembovska et al., 2017) concerning
386 lightweight alkali activated material using different waste (metakaolin, aluminum scrap,
387 glass and steel plant wastes) showed densities between 380-470 kg/m^3, open porosities in
388 the range 27-30% and compressive strength between 1.1-2 MPa. Zhang et al (Zhang et al.,
389 2015) prepared geopolymer foam concretes with fly ashes and foaming agents. Densities
390 were around 1000 kg/m^3 and compressive strength between 7-10 MPa. As can be seen, the
391 results obtained in the current work are in the same range of the geopolymers described in
392 those studies.

393 **3.5. Acoustic properties**

Figure 4 shows the acoustic absorption (α) versus frequency for the four tested geopolymers. The coefficients of variation were less than 9 %.

In general, all curves showed a broad peak at low frequencies (1-2000 Hz), followed by a drop and finally a rise from 3500-4000 Hz. The main characteristic of the curves is the high absorption at frequencies less than 2000 Hz, which are the traffic noise frequencies (road transportation vehicles such as saloon, utility vehicle, small car, large car, articulated truck and bus) (Berglund and Hassmen, 1996). The curves also show great absorption at high frequencies, which are characteristic of noise from impulsive sources such as jack hammering or pile driving (Berglund and Hassmen, 1996).

Figure 4. Acoustic absorption

The effect of Paval is clear: an increase in acoustic absorption is observed in all frequency ranges. The effect of temperature setting also affects the acoustic absorption but it is more apparent at low (less than 1500 Hz) and high (more than 3000 Hz) frequencies. These results are in good agreement with the porosities. As previously mentioned, acoustic properties are closely linked with the porous structure of the porous geopolymers since the sound absorption is closely associated with the friction-energy loss in the wall of pores in a porous material (Arenas et al., 2017). More specifically, the sound absorption coefficient of a porous geopolymer is related to the porosity, pore size, tortuosity and permeability in the pore network through which acoustic energy can travel and be attenuated inside the material (Arenas et al., 2017b). Porous geopolymers obtained in this work presented porosities in the range 12-22 %, that is, relatively low porosities. It is well known that regarding porosity, only open porosity is beneficial to acoustic properties, but if the open

417 porosities are very high, the impact of sound in the walls of the porous structure is reduced,
418 diminishing its sound absorption (Maderuelo-Sanz et al., 2016). Regarding pore size, pore
419 sizes of geopolymers obtained in this work are between 1-7 mm (see Figure 3). Some
420 authors (Park et sl., 2005, Flores, 1990) revealed that the sound absorption between 100
421 and 5000 Hz is produced by pore sizes between 1 and 5 mm. Concerning tortuosity, Figure
422 3e (cross section of FA50-PV50 geopolymer) shows the macro-tortuous structure of the
423 geopolymer, which increases the impact of the sound in the wall of the channels since the
424 wave is finding a network with long, open and tortuous channels to dissipate. With regard
425 to permeability, it should be taken into account how the wave penetrates in the material. As
426 commented upon in section 2.3.4, the incident sound wave in the sound absorption test
427 penetrates through the more porous zone (upper zone Figure 3e) to the less porous zone
428 (bottom zone Figure 3e), that is, the waves pass through great pores interconnected with
429 small pores that close the way and so the waves are reflected and must travel through the
430 channels again, increasing the dissipation of sound energy (Arenas et al., 2015). Therefore,
431 taking these arguments into account, it is feasible that the porous geopolymers obtained in
432 this work, although they presented low porosities, show great acoustic absorption, even in
433 comparison with other highly porous materials (Bujoreanu et al., 2017).

434 In order to numerically visualize the values of sound absorption, the Noise Reduction
435 Coefficients (NRC) were calculated as 0.148 for geopolymer FA100-PV0 (40 ºC), 0.221
436 for FA75-PV25 (40 ºC), 0.251 for FA50-PV50 (40 ºC) and 0.351 forFA50-PV50 (70 ºC).

437 **3.3. Leaching test**

438 Results of NEN 7375 as cumulative concentration at 64 days for tested geopolymer are
439 detailed in Table 4. The Dutch Decree on Soils Quality limits are also listed.

440 Table 4. NEN 7375 results

441

442 As can be seen, Ba, Cd, Co, Hg, Ni, Pb, Sn and Zn are under the detection limit of the
443 analytical technique. The setting temperature did not significantly affect the leaching results
444 since cumulative concentration remains practically constant as temperature changed. The
445 reduction of As and V concentration in leachates as PV content increased in the matrix was
446 noteworthy. This is mainly due to the high concentration of As and V in the fly ash. On the
447 contrary, Cr, Cu, Sb and Mo concentrations increased as PV content increased, which is
448 due to two factors. The first factor is the high content of these metals in Paval. The second
449 factor is the great leaching-exposed surface of samples with more PV content since these
450 samples presented higher porosity (see Figure 3). In any case, the Paval by-product
451 contains large amounts of Zn, Cr, Cu, Ni, Sn and Se, which appear in low levels in the
452 geopolymeric matrix, which suggests a great immobilization degree of those metals in the
453 geopolymer. In addition, the fifteen analyzed metals in the four geopolymer materials fulfill
454 the DSQ limits. Therefore, the manufacturing materials could be used as moulded-building
455 material in accordance with the Dutch Decree.

456 **3.7. Comparison with other porous geopolymeric materials**

457 The physical, mechanical and acoustic results were compared with those obtained in other
458 works. Zhang et al (Zhang et al., 2015) prepared geopolymer foam concrete (as described

459 in Section 3.4) with densities and compressive strength similar to the current work. They
460 showed a high sound absorption in the frequencies 40-150 Hz. Our porous geopolymers
461 (those prepared with paval) showed the highest sound absorption in medium frequency
462 sound (650-1600 Hz). Hung et al (Hung et al., 2014) manufactured inorganic polymeric
463 foam with metakaolin and blast furnace slag using different foaming agent (air bubbles)
464 dosages. Densities obtained were in the range 0.4-1 g/cm^3 and compressive strengths
465 between 7-11 MPa. Their sound absorption curves are different, without peaks and they are
466 in ascending order with the frequencies. The geopolymer with 1 g/cm^3 of density (the same
467 as the geopolymer FA50-PV50 70ºC) showed sound absorption coefficients between 0.1-
468 0.2 (lower than ours). Geopolymers prepared by Papa et al (Papa et al., 2016) contained
469 metakaolin as a geopolymer raw material and silica fume as a pore generating agent and
470 were activated with two types of activating solutions (Na or K sodium-silicate). The K
471 activated geopolymer showed 0.59 g/cm^3 density and open porosities of 50 %. Sound
472 absorption coefficient curves were similar to those in this study but with two higher peaks
473 (0.8-0.9) in the same frequencies as here. A previous study by the authors (Luna-Galiano et
474 al., 2018) studied the porous geopolymer manufactured using fly ash (geopolymerization
475 precursor) and silica fume (pore generation agent). The porous geopolymer prepared with
476 fly ash and silica fume in a proportion of 60-40 in weight (similar to the composition of
477 FA50-PV50), set a 40 ºC, showed an open porosity of 28 %, compressive strength of 6.9
478 MPa and NRC of 0.21. The geopolymer FA50-PV50 set at 40 ºC showed an open porosity
479 of 15 %, compressive strength of 4.3 MPa and NRC of 0.25. The results have also been
480 compared with a conventional porous concrete (CPC) which was prepared using an
481 Ordinary Portland Cement (CEM II/B-L32,5N) and coarse aggregates (CA) in a proportion

of OPC II: 20/CA: 80 (Arenas et al., 2017). The open void ratio of the CPC was 26%, the compressive strength at 28 days was 4.5 MPa and the obtained NRC was 0.26. As can be seen, all the materials show similar mechanical and acoustic properties.

4. CONCLUSIONS

The aim of this work is to analyse how the introduction of Paval (an aluminum industry waste stream) in a carbon combustion fly ash based geopolymer can produce a porous geopolymerwith noise-absorbing properties and characterize this porous material. Setting time, volume expansion, open porosity, compressive strength and noise absorption were evaluated taking into account the fly ash-Paval ratio and the setting temperature. To increase the Paval content up to 50 %wt and to increase the setting temperature from 40 to 70 ºC accelerated setting of the geopolymer and increased the gas hydrogen release, thus enhancing volume expansion of the material. Consequently, the open porosity was increased and therefore the acoustic properties were significantly improved. As the fly ash and Paval used raised certain leaching concerns with respect to Cr, Mo and Se, the geopolymers were subjected to the tank leaching test NEN 7375. The final results met the limits for the Dutch Decree on Soils quality, so the Cr, Mo and Se problem was resolved.

Acknowledgements

Authors would like to acknowledge the help received by CITIUS (General Research Services) from University of Seville, especially the XRD laboratory.

Compliance with Ethical Standards:

Authors declare that they have no conflicts of interest.

Funding

This research did not receive any specific grant from funding agencies in the public, commercial, or not-for-profit sectors.

References

-Ahmed, S., Saurikhia, A., Haleem, A., Gangopadhyay, S. 2016. Geographical spread of fly ash generation and residual potential for its utilization in India. International Journal of Innovative Research and Review. ISSN: 2347 – 4424. 4 (1), 8-19 http://www.cibtech.org/jirr.htm

-Ahmer Ali Siyal, Khairum Azizi Azizli, Zakaria Man, Hafeez Ullah., 2016. Effects of parameters on the setting time of fly ash based geopolymers using Taguchi Method. Pro. Eng. 148, 302-307. DOI: 10.1016/j.proeng.2016.06.624

-Al Bakri, M., A.M., Kamarudin. H., Bnhussain. M., Khairul Nizar, I., Mastura, W.I.W., 2011. Mechanism and chemical reaction of fly ash geopolymer cement- A review. Asian J. Sci. Res. 1(5), 247-253.

-Arellano Aguilar, R., Burciaga Díaz, O., Escalante García, J.I., 2010. Lightweight concretes of activated metakaolin-fly ash binders with blast furnace slag aggregates. Constr. Build. Mater. 24(7), 1166-1175. https://doi.org/10.1016/j.conbuildmat.2009.12.024

-Arenas, C., Leiva, C., Vilches, L.F., Cifuentes, H., Rodríguez-Galán, M. 2015. Technical specifications for highway noise barriers made of coal bottom ash-based sound absorbing

523 concrete. Constr. Build. Mater. 95, 585-591.
524 https://doi.org/10.1016/j.conbuildmat.2015.07.107
525 -Arenas, C., Luna-Galiano, Y., Leiva, C., Vilches, L.F., Arroyo, F., Villegas, R.,
526 Fernández-Pereira, C., 2017. Development of a fly ash-based geopolymeric concrete with
527 construction and demolition wastes as aggregates in acoustic barriers. Constr. Build. Mater.
528 134, 433–442. https://doi.org/10.1016/j.conbuildmat.2016.12.119
529 -Arenas, C., Leiva, C., Vilches, L.F., González Ganso, J.A. 2017. Approaching a
530 methodology for the development of a multilayer sound absorbing device recycling coal
531 bottom ash. Appl. Acoust. 115, 81-87. https://doi.org/10.1016/j.apacoust.2016.08.021
532 -ASTM C 618-05: 2005. Standard Specification for Coal Fly Ash and Raw or Calcined
533 Natural Pozzolan for Use in Concrete. ASTM International. USA.
534 -ASTM D3682-78: 1983. Test method for mayor and minor elements in coal and coke ash
535 by atomic absorption. ASTM International. USA.
536 -Bai, C., Colombo, P. 2018. Processing, properties and applications of highly porous
537 geopolymers: a review. Ceram. Int. 44(14). 16103-16118
538 https://doi.org/10.1016/j.ceramint.2018.05.219
539 -Bai, C., Li, H., Bernardo, E., Colombo, P. 2019. Waste-to-resource preparation of glass-
540 containing foams from geopolymers. Ceram. Int. 45(6), 7196-7202
541 https://doi.org/10.1016/j.ceramint.2018.12.227
542 -Basque Eco Design Meeting. 2017. Cierre del ciclo del Aluminio desarrollando nuevas
543 soluciones de valor.
544 -Berglunda, B., Hassme´n, P., 1996. Sources and effects of low-frequency noise. J. Acoust.
545 Soc. Am. 99(5), 2985-3002. DOI: 10.1121/1.414863.

-Bujoreanu, C., Nedeff, F., Benchea, M., Agop, M. 2017. Experimental and theoretical considerations on sound absorption performance of waste materials including the effect of backing plates. Appl. Acoust., 119, 88-93. https://doi.org/10.1016/j.apacoust.2016.12.010

-Cilla, M.S., Morellia, M.R., Colombo, P., 2014. Open cell geopolymer foams by a novel saponification/peroxide/gelcasting combined route. J. Eur. Ceram. Soc. 34(12), 3133–3137. https://doi.org/10.1016/j.jeurceramsoc.2014.04.001

-Davidovits, J., 1991. Geopolymers: inorganic polymeric new materials. J. Therm. Anal. 37, 1633-1656. https://doi.org/10.1007/BF01912193

-De Silva, P., Sagoe-Crenstil, K., Sirivivatnanon, V., 2007. Kinetics of geopolymerization: Role of Al_2O_3 and SiO_2. Cem. Concr. Res. 37(4), 512-518. https://doi.org/10.1016/j.cemconres.2007.01.003

-Dembovska, L., Bajare, D., Ducman, V., Korat, L., Bumanis, G. 2017. The use of different by-products in the production of lightweight alkali activated building materials. Constr. Build. Mater. 135. 315-322. https://doi.org/10.1016/j.conbuildmat.2017.01.005

-Digne, M., Sautet, P., Raybaud, P., Toulhoat, H., Artacho, E., 2002. Structure and stability of aluminium hydroxides: a theoretical study. J. Phys. Chem. B 106, 5155-5162. DOI: 10.1021/jp014182a

-DSQ (Decree on Soil Quality). Staatsblad 2007. Besluit van 22 november 2007. hHoudende regels inzake de kwaliteit van de bodem (Besluit bodemkwaliteit). Staatsblad. 2007. nr 469.

-EN 1097-7: 2009. Tests for mechanical and physical properties of aggregates - Part 7: Determination of the particle density of filler - Pyknometer method.

-EN 1936:2006. Natural stone test methods - Determination of real density and apparent density and of total and open porosity.

-EN 196-1:2006. Methods of testing cement - Part 1: Determination of strength. European committee for standarisation. Brussels. Belgium.

-EN 196-3: 2005. Methods of testing cements: Part 3. Determination of setting times and soundness. CEN (European Committee for Standardization), Brussels, Belgium.

-EN ISO 10534-2: 1998. Acoustics determination of sound absorption coefficient and impedance or admittance by the impedance tube. Part II: Transfer function method.

-Fernández-Jiménez, A., Palomo, A., 2003. Characterization of fly ashes. Potential reactivity as alkaline cements. Fuel. 82(8), 2259-2265. https://doi.org/10.1016/S0016-2361(03)00194-7

-Fernández-Jiménez, A., Palomo, A., Criado, M., 2006. Alkali activated fly ash binders. A comparative study between sodium and potassium activators. Mater. Construcc. 56(281), 51-65. DOI.:10.3989/mc.2006.v56.i281.92.

-Flores, P., 1990. Manual de Acústica, Ruidos y Vibraciones, GYC (eds).

-Font, A., Borrachero, M.V., Soriano, L. 2017. Geopolymer eco-cellular concrete (GECC) based on fluid catalytic cracking catalyst residue (FCC) with addition of recycled aluminium foil powder. J. Clean. Prod. 168. 1120-1131. https://doi.org/10.1016/j.jclepro.2017.09.110

-Geoash: Undertanding and mastering coal fired ashes geopolymerization process in order to turn potential into profit. 2004-2007. Research Fund for Coal and Steel of the European Community. RFC-CR-04005.

-García Serrada, C., 2002. Utilización de Paval como filler de aportación para la fabricación de mezclas bituminosas en caliente. Carreteras: Revista técnica de la Asociación Española de la Carretera. 81-92.

-Gonzalo Delgado, L., 2008. Obtención y caracterización de bohemita a partir de un residuo peligroso de la industria del aluminio. Universidad compútense de Madrid. Departamento de Cristalografía y Mineralogía. Madrid.

-Gonzalo Delgado, L., López-Delgado, A., López Gómez, F.A., Alguacil, F.J., López-Andrés, S., 2011. Recycling of hazardous waste from tertiary aluminium industry in a value-added material. Waste. Manag. Research. 29(2), 127-134. http://dx.doi.org/10.1177/0734242X10378330

-Hajimoohammadi, A., Ngo, T., Mendis, P., Sanjayan, J., 2017. Regulating the chemical foaming reaction to control the porosity of geopolymer foams. Mater. Design. 120, 255-265. https://doi.org/10.1016/j.matdes.2017.02.026

-Han, F., Seiffert, G., Zhao, Y., Gibbs, B., 2003, Acoustic absorption behaviour of an open-celled aluminium foam. J. Phys. D.: Appl. Phys. 36, 294–302. http://stacks.iop.org/0022-3727/36/294/d30312.pdf;http://www.iop.org/

-Hassan, H. S., Abdel-Gawwad, H. A., García, S. V., Israde-Alcántara, I. 2018. Fabrication and characterization of thermally-insulating coconut ash-based geopolymer foam. Waste. Manag. 80, 235-240. https://doi.org/10.1016/j.wasman.2018.09.022

-Henon, J., Alzina, A., Absi, J., Smith, D.S., Rossignol, S., 2013. Potassium geopolymer foams made with silica fume pore forming agent for thermal insulation. J. Porous. Mater. 20(1), 37-46. DOI: 10.1007/s10934-012-9572-3

612 -Hlaváček, P., Šmilauer, V., Škvára, F., Kopecký, L., Šulc, R., 2015. Inorganic foams made
613 from alkali-activated fly ash: Mechanical chemical and physical properties. J. Eur. Ceram.
614 Soc. 35(2), 703-709. https://doi.org/10.1016/j.jeurceramsoc.2014.08.024
615 -Kamseu, E., Nait-Ali, B., Bignozzi, C., Leonelli, C., Rossignol, S., Smith, D.S. 2012. Bulk
616 composition and microstructure dependence of effective thermal conductivity of porous
617 inorganic polymer cements. J. Eur. Ceram. Soc. 32, 1593-1603.
618 https://doi.org/10.1016/j.jeurceramsoc.2011.12.030
619 -Kränzlein, E., Pöllmann, H., Krcmar, W. 2018. Metal powders as foaming agents in fly
620 ash based geopolymer synthesis and their impact on the structure depending on the Na/Al
621 ratio. Constr. Build. Mater. 90, 161-168.
622 https://doi.org/10.1016/j.cemconcomp.2018.02.009
623 -López-Delgado, A.. Tayibi, H., Pérez, C., Alguacil, F.J., López, F.A., 2009. A hazardous
624 waste from secondary aluminium metallurgy as a new raw material for calcium aluminate
625 glasses. J. Hazard. Mater. 165(1–3), 180-186.
626 https://doi.org/10.1016/j.jhazmat.2008.09.124
627 -López Gómez, F.A., 2005. Patent nº ES 2 197 797 B1 Spain.
628 -Luna-Galiano, Y., Fernández-Pereira, C., Izquierdo, M., 2016. Contributions to the study
629 of porosity in fly ash-based geopolymers. Relationship between degree of reaction, porosity
630 and compressive strength. Mater. Construcc. 66(324).
631 http://dx.doi.org/10.3989/mc.2016.10215
632 -Luna-Galiano, Y., Leiva, C., Arenas, C., Fernández-Pereira, C., 2018. Fly ash based
633 geopolymeric foams using silica fume as pore generation agent. Physical, mechanical and
634 acoustic properties. J. Non-Cry. Sol. 500, 196-204.

https://doi.org/10.1016/j.jnoncrysol.2018.07.069

-Maderuelo-Sanz, R., Nadl-Gisbert, A., Crespo-Amorós, J.E., Barrigón-Morillas, J.M., Parrés-García, F. 2016. Influence of the Microstructure in the Acoustical Performance of Consolidated Lightweight Granular Materials. Acoust. Aust. 44,149-157. https://doi.org/10.1007/s40857-016-0048-5

-Masia, G., Rickard, W.D.A., Vickers, L., Bignozzi, M.C., van Riessen, A., 2014. A comparison between different foaming methods for the synthesis of light weight geopolymers. Ceram. Int. 40(9) Part A, 13891–13902. https://doi.org/10.1016/j.ceramint.2014.05.108

-Mohammadian, M., Haghi, A.K., 2013. A study on application of recycled thermosetting plastic. Rev. Rom. Mater. 43(3), 276-284.

-NEN 7375 leaching test. 2005. Leaching Characteristics of Moulded or Monolithic Building and Waste Materials. Determination of Leaching of Inorganic Components with the Diffusion Test. The tank test. NNI (Netherlands Normalization Institute Standard). Delft. The Netherlands.

-Neville, A.M., 2011. Properties of concrete. Fifth eds. London. UK. Pearson.

-Papa, E., Medri, V., Kpogbemabou, D., Morinière V., Laumonier J., Vaccari, A., Rossignol, S. 2016. Porosity and insulating properties of silica-fume based foams, Energy Build. 131, 223-232. https://doi.org/10.1016/j.enbuild.2016.09.031

- Park, B., Seo, D.S., Lee, J. 2005. Studies on the sound absorption characteristics of porous concrete based on the content of recycled aggregate and target void ratio. Cement. Concrete. Res. 35(9), 1846-1854. https://doi.org/10.1016/j.cemconres.2004.12.009

-Pereira Antunes, M.L., Souza Santos, H., Souza Santos, P., 2002. Characterization of the aluminium hydroxide microcrystals formed in some alcohol-water solutions. Mater. Chem. Phy. 76, 243-249. https://doi.org/10.1016/S0254-0584(01)00535-1

-Prud'homme, E., Michaud, P., Joussein, E., Peyratout, C., Smith, A., Arrii-Clacens, S., Clacens, J.M., Rossignol, S., 2010. Silica fume as porogent agent in geo-materials at low temperature. J. Eur. Ceram. Soc. 30(7),1641-1648. https://doi.org/10.1016/j.jeurceramsoc.2010.01.014

-Prud'homme, E., Michaud, P., Joussein, E., Peyratout, C., Smith, A., Rossignol, S., 2011. In situ inorganic foams prepared from various clays at low temperature. Appl. Clay. Sci. 51(1–2), 15-22. https://doi.org/10.1016/j.clay.2010.10.016

-Schmäh, H., 1946. Simple preparation of well-crystallized bayerite. Zeitschrift fürNaturforschung. 1(6), 323-324.

-Tayibi, N., Pérez, C., López, F.A., López-Delgado, A., 2005. Evolución de las propiedades mecánicas de un residuo de la metalurgia secundaria del aluminio estabilizado con yeso. Rev. Metal. 41(4), 280-285. http://revistademetalurgia.revistas.csic.es

-Xu, F., Gu, G., Zhang, W., Wang, H., Huang, X., & Zhu, J. 2018. Pore structure analysis and properties evaluations of fly ash-based geopolymer foams by chemical foaming method. Ceram. Int. 44(16), 19989-19997. https://doi.org/10.1016/j.ceramint.2018.07.267

-Zhang, Z., Provis, J.L., Reid, A., Wang, H., 2014. Geopolymer foam concrete: An emerging material for sustainable construction. Constr. Build. Mater. 56, 113-127. https://doi.org/10.1016/j.conbuildmat.2014.01.081

679 Table 1. Chemical composition of FA and PV

	Moisture (%)	LOI 750ºC	Chemical composition (wt %)						
			Fe_2O_3	CaO	MgO	SiO_2	Al_2O_3	Na_2O	K_2O
FA	0.05	3.32	5.86	3.94	1.84	63.9	21.5	0.68	1.67
PV	4.58	8.62	2.45	3.06	5.87	11.4	75.9	1.61	0.88

680

681 Table 2. Minor elements and metal concentrations obtained after UNE EN 12457-4 leaching test of FA and PV

	Minor elements ($mg \cdot kg^{-1}$)														
	As	Ba	Cd	Co	Cr	Cu	Hg	Mo	Ni	Pb	Sb	Se	Sn	V	Zn
FA	24	1287	3	33	167	97	0,08	17	102	47	6	19	6	248	136
PV	16	2794	<2	18	802	3550	<1	74	320	322	15,3	562	62	160	2056
	UNE-EN 12457 ($mg \cdot kg^{-1}$)														
	As	Ba	Cd	Co	Cr	Cu	Hg	Mo	Ni	Pb	Sb	Se	Sn	V	Zn
FA	<0.05	0.37	<0.005	<0.005	0.53	<0.03	<0.05	1.1	<0.01	<0.05	<0.01	0.19	<0.05	<0.01	<0.001
PV	<0.05	0.52	<0.01	<0.01	0.02	<0.015	<0.005	2.49	<0.05	<0.015	0.216	0.091	<0.01	0.37	0.08
IW-EULFD	0.5	20	0.04		0.5	2	0.01	0.5	0.4	0.5	0.06	0.1			4
NHW-EULFD	2	100	1		10	50	0.2	10	10	10	0.7	0.5			50
HW-EULFD	25	300	5		70	100	2	30	40	50	5	7			200

682

683 Table 3. Open porosity and compressive strength

	Open porosity (%)	Bulk density (kg/m^3)	Compressive strength (MPa)
FA100-PV0 40ºC	10.0 ± 0.9	1640 ± 24	14.8 ± 1.7
FA75-PV25 40ºC	11.9 ± 1.0	1238 ± 18	5.32 ± 0.6
FA50-PV50 40ºC	14.9 ± 1.3	1056 ± 32	4.23 ± 0.3
FA50-PV50 70ºC	21.9 ± 2.2	916 ± 27	3.07 ± 0.4

684

685

686 Table 4. NEN 7375 results

	Cumulative concentration (mg/m^2)				DSQ limits
	FA-PV 100-0	FA-PV 75-25	FA-PV 50-50	FA-PV 50-50 70ºC	mg/m^2
As	3.78	2.05	1.49	1.28	260
Ba	<0.07	<0.07	<0.10	<0.07	1500
Cd	<0.07	<0.07	<0.07	<0.07	3.8
Co	<0.07	<0.07	<0.07	<0.07	60
Cr	0.31	0.96	2.61	2.65	120
Cu	0.12	0.55	2.49	2.74	98
Hg	<0.07	<0.07	<0.07	<0.07	1.4
Mo	1.03	2.34	3.41	3.27	144
Ni	<0.07	<0.07	<0.07	<0.07	81
Pb	<0.07	<0.07	<0.07	<0.07	400
Sb	0.23	0.34	0.62	0.69	8.7
Se	2.65	2.24	2.66	2.35	4.8
Sn	<0.07	<0.07	<0.07	<0.07	50
V	28.58	19.75	11.21	11.43	320
Zn	<0.36	<0.36	<0.37	<0.36	800

687

688

689

690

691

692 Figure 1. XRD patterns of FA, PV and geopolymers FA100-PV0 and FA50-PV50

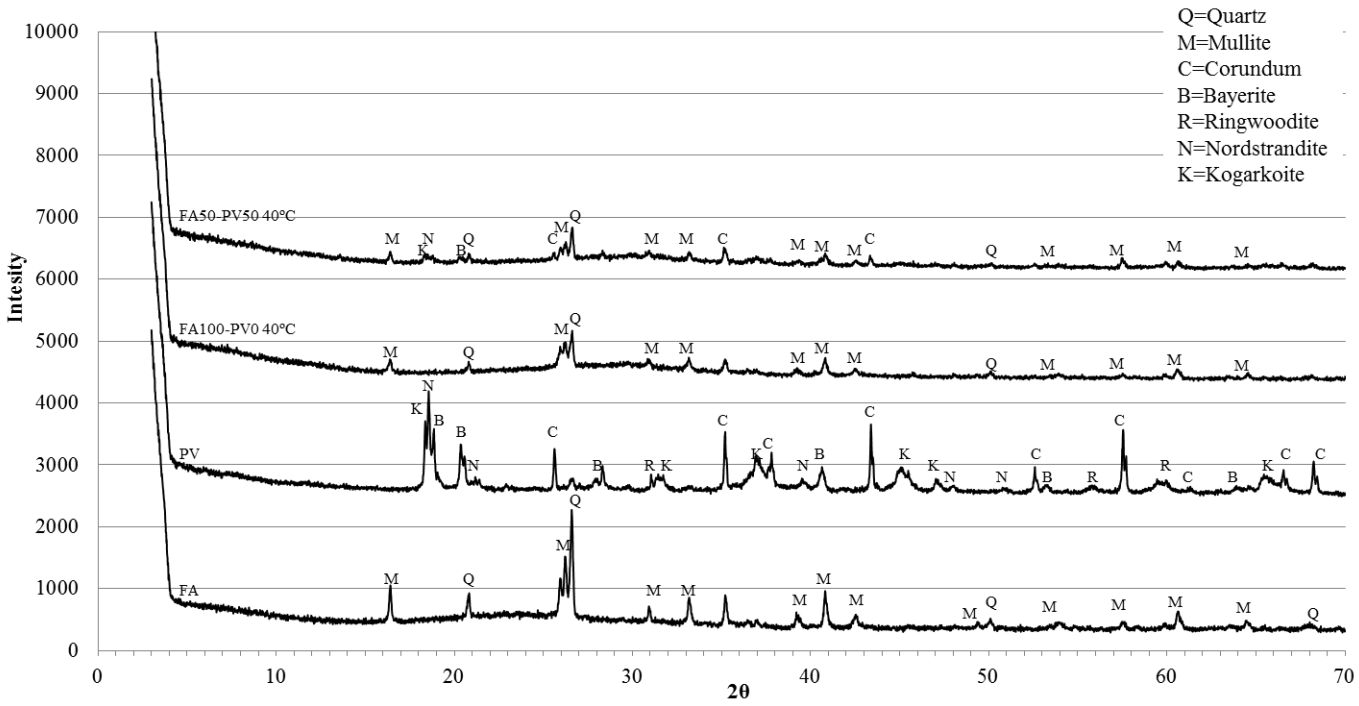

693

694 Figure 2. Expansion volume and setting curves

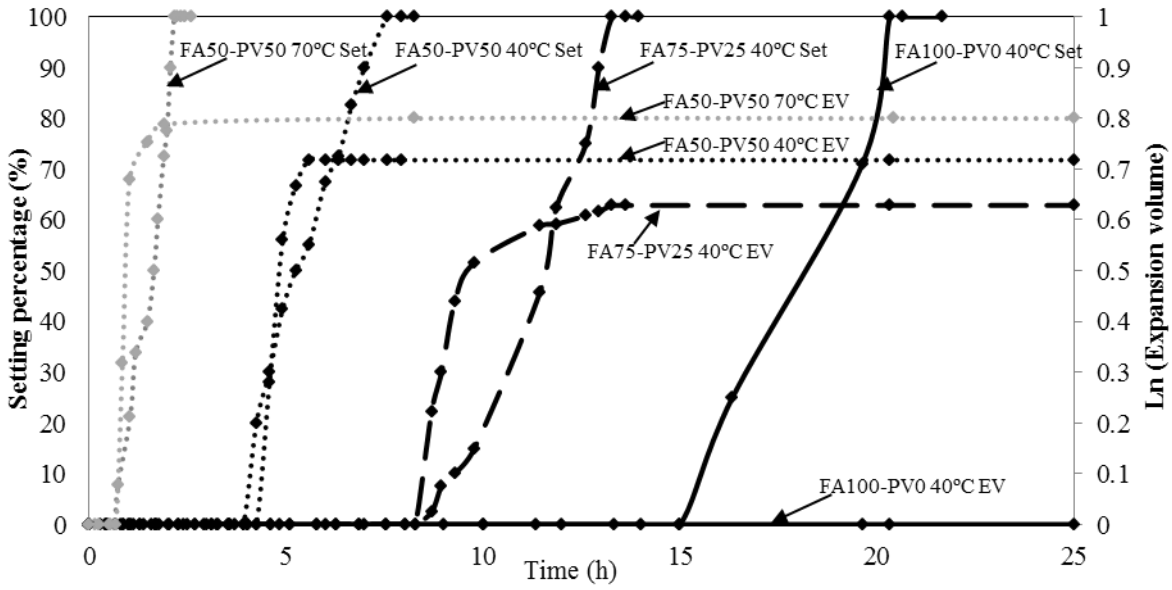

695

696

Figure 3. Geopolymer images and cross section of FA50-PV50 70ºC

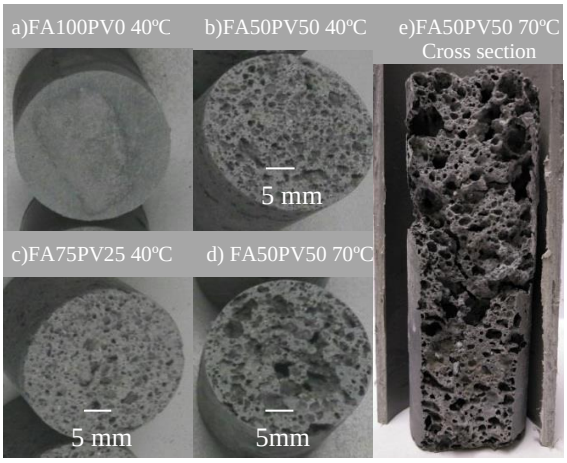

Figure 4. Acoustic absorption